# Thermodynamic Mechanisms and Parametric Landscape Design for Urban Water Bodies in Local Thermal and Humid Environment Regulation

Cuixia Ma

School of Architecture, Nanyang Institute of Technology, Nanyang 473000, China

Corresponding Author Email: 3072041@nyist.edu.cn

**ABSTRACT**

The intensification of the urban heat island effect exacerbates the imbalance of local thermal and humid environments, making the thermodynamic regulation function of urban water bodies a key approach for microclimate optimization. However, current research faces core issues, including the disconnection between thermodynamic mechanisms and landscape parameter control, as well as the unclear multi-scale transfer laws. This study takes urban water bodies in typical climatic regions as the research object, using pilot case remote sensing analysis to identify phenomena and key parameters. It combines field observations, indoor control experiments, and numerical simulations based on coupled thermodynamic equations to systematically analyze the thermodynamic mechanisms of water-body thermal and humidity regulation, incorporating landscape parameters. A multi-scale collaborative parametric system for landscape design is constructed and case verification is carried out. Thermodynamic optimization practices in a residential area in Guangzhou demonstrate that optimization based on the multi-scale parametric system can significantly improve the regional thermal and humid environment. The daytime peak temperature drops by 2.3°C, relative humidity increases by 6.2 percentage points, latent heat flux increases by 49.5%, and the proportion of latent heat flux to net radiation flux rises to 63.5%. After optimization, the daytime peak index PET drops from 41.5°C to 34.8°C, significantly improving thermal comfort, and the thermodynamic efficiency increases by 42.3%. The simulation results show small deviations from field observations, validating the scientific and practical feasibility of the proposed plan. This study establishes a deep-coupled analysis framework of landscape parameters-thermodynamic processes-thermal and humidity effects, providing theoretical support and engineering solutions for precise thermodynamic control of urban microclimates.

## 1. INTRODUCTION

The combined effects of global urbanization and climate change have significantly intensified the urban heat island effect [1-3], causing imbalances in local thermal and humid environments [4], which pose severe threats to human comfort, building energy efficiency, and the stability of urban ecosystems. Against this backdrop, precise microclimate regulation based on thermodynamic principles [5, 6] has become a key breakthrough for mitigating the heat island effect and optimizing urban living environments. Urban water bodies, as natural thermodynamic regulators of local thermal and humid environments [7, 8], redistribute energy and mass through key thermodynamic processes such as evaporation phase change, radiation exchange, and convective diffusion. Their application potential in alleviating the heat island effect has received widespread attention. However, existing studies still face core bottlenecks: insufficient coupling between thermodynamic mechanism analysis and landscape design parameters [9], which often focuses on surface-level observations and parameter associations, lacking in-depth research on process-parameter-effect coupling from a

thermodynamic perspective; meanwhile, multi-scale thermodynamic transfer laws remain unclear [10], resulting in a lack of systematization in landscape parameterization design systems, making it difficult to meet the need for precise thermodynamic control in engineering practice.

A review of domestic and international research progress shows that the thermodynamic fundamental research on thermal and humidity regulation by urban water bodies has focused on the application and modification of energy balance equations in water body-atmosphere systems, as well as quantitative models for phase changes and heat transfer processes. However, existing results still have notable limitations in multi-process coupling simulations and multi-scale linkage analysis. In research on the correlation between water bodies and landscape parameters, scholars have focused on the impact of landscape parameters such as morphology, configuration, and attributes on thermal and humidity effects [11-13], but there is a common issue of disconnect between thermodynamic mechanisms and parameter control, failing to reveal the intrinsic thermodynamic paths through which parameters affect thermal and humidity effects. Although multi-scale microclimate regulation studies have discovered

differences in urban water body thermal and humidity regulation effects at different scales [14, 15], the current parameterization system still lacks scientific scale division and clarity in cross-scale transfer mechanisms. In summary, existing research has not formed a complete research system centered on thermodynamic principles, coupled with landscape parameters, and spanning multiple scales. This research gap provides a clear academic entry point and core exploration direction for this study.

Based on the above research background and existing shortcomings, this study proposes three core scientific questions: First, in the cooling and humidifying effects of urban water bodies in typical climatic regions, what is the relative proportion of contributions from evaporation latent heat and radiation regulation, and what are the landscape parameters that dominate and their corresponding thermodynamic control thresholds? Second, how do single or combined landscape parameters regulate the energy flux distribution at the water-atmosphere interface through thermodynamic pathways, and what are the thermodynamic synergistic or antagonistic mechanisms under multi-parameter interactions? Third, what are the thermodynamic transfer laws at the micro-interface, meso-patch, and macro-network scales, and how do the dominant thermodynamic mechanisms and core design parameters match at different scales? The core objective of this study is to systematically reveal the thermodynamic mechanisms of water body thermal and humidity regulation coupled with landscape parameters, elucidate multi-scale thermodynamic transfer laws, and construct a multi-scale collaborative landscape parameterization system to provide scientific basis and technical support for precise thermodynamic control of urban microclimates.

To achieve the above research objectives, this study adopts a multi-method integration technical approach, including pilot case analysis, field observation experiments, indoor control experiments, numerical simulation, and thermodynamic mechanism analysis with statistical modeling. The overall technical route follows the logical chain of "pilot case identification of phenomena → theoretical foundation construction → coupling parameter mechanism analysis → multi-scale parameterization system construction → case verification application", clarifying the thermodynamic analysis focus and technical method connection at each research stage, ensuring the systematic and scientific nature of the research process.

The subsequent chapters of this paper are arranged as follows: Chapter 2 verifies the thermal and humidity regulation effects of water bodies through pilot case studies and proposes core scientific hypotheses; Chapter 3 conducts thermodynamic process observations and mechanism analysis of coupled landscape parameters; Chapter 4 constructs a multi-scale collaborative landscape parameterization system; Chapter 5 verifies the effectiveness of the parameterization system through case applications; and finally, the research results and scientific value are summarized through discussions and conclusions. The innovations of this research are mainly reflected in four aspects: first, based on empirical analysis of pilot cases, the research starting point is elevated from literature gaps to observational phenomena and scientific hypotheses, enhancing the rigor of the research logic; second, a deep-coupled analysis framework of landscape parameters-thermodynamic processes-thermal and humidity effects is constructed, analyzing parameter regulation mechanisms from

the thermodynamic principle level, breaking through the research bottleneck of mechanism-parameter disconnect; third, multi-scale thermodynamic transfer laws are clarified, and a parameterization system with precise matching for each scale is established, improving the systematization and thermodynamic control targeting of the design system; fourth, thermal and humidity optimization design guidelines are generated for different climatic regions and scales, achieving efficient translation of theoretical results into engineering practice.

## 2. PILOT CASE STUDY AND CORE HYPOTHESIS

### 2.1 Case selection and data sources

To accurately identify the fundamental characteristics and key influencing factors of urban water bodies' thermal and humidity regulation, this study selects two types of typical urban water bodies as pilot cases: East Lake in the subtropical monsoon climate zone and a river section of the Hunhe River in the temperate continental climate zone. The case selection follows the principles of typicality and comparability: East Lake is surrounded by parkland and low-density residential areas, while the Hunhe River section is surrounded by high-density commercial and industrial areas. These two cases cover different water body forms, climate backgrounds, and built environment gradients, which effectively isolate the interference of climate and underlying surface differences on water body thermal and humidity effects.

The data system is built around remote sensing inversion data and open-source data, forming an analysis foundation supported by multi-source data collaboration. The surface temperature data is sourced from Landsat8/9 OLI/TIRS sensor images with a spatial resolution of 30m. The time span is selected from the summer heat period to the winter cold period between 2020 and 2023, obtaining 48 valid images to extract temperature differences between water bodies and surrounding underlying surfaces. Meteorological data is obtained from ERA5-Land hourly reanalysis data, including parameters such as 2m air temperature, relative humidity, and 10m wind speed, with a spatial resolution of 0.1°×0.1°, which supplements the regional meteorological background field. Land use and built environment data come from GlobeLand30 global land cover data. Landscape parameters, such as built-up area density and vegetation coverage, are extracted to construct a landscape parameter dataset. All data are processed to standardize coordinate systems and time scales, ensuring data consistency.

### 2.2 Rapid analysis methods and process

Data preprocessing focuses on improving temperature inversion accuracy and spatial-temporal matching. The remote sensing image preprocessing process includes radiometric calibration, atmospheric correction, and surface temperature inversion: atmospheric correction uses the 6S model to eliminate atmospheric scattering and absorption effects. The surface temperature inversion for Landsat8/9 data uses the split-window algorithm, with the core formula being:

$$T_s = a_0 + a_1 T_{10} - a_2 T_{11} + (b_0 + b_1 T_{10} - b_2 T_{11})\frac{1}{\cos\theta} + c_0 \qquad (1)$$

where, $T_s$ is the surface temperature, $T_{10}$ and $T_{11}$ are the

brightness temperatures of bands 10 and 11, $\theta$ is the solar zenith angle, and $a_0$, $a_1$, $a_2$, $b_0$, $b_1$, $b_2$, $c_0$ are the algorithm coefficients. The temperature inversion results are verified through field synchronous observation data, with a root mean square error (RMSE) ranging from 0.85 to 1.23 K, meeting the analysis accuracy requirements. The open-source meteorological data and remote sensing data are spatially matched using linear interpolation, and the time series are processed with a moving average method to eliminate short-term fluctuations.

Rapid analysis adopts a progressive method system of "range definition - correlation identification - contribution decomposition." The buffer zone analysis is based on the water body boundary, setting four gradient buffer zones: 0–50 m, 50–100 m, 100–200 m, and 200–500 m. The temperature difference between the average temperature of each buffer zone and the control zone is used to define the cooling effect range of the water body. Correlation analysis uses the Pearson correlation coefficient method to quantify the correlation strength between 12 landscape parameters, such as water body area, shoreline complexity, and built-up density, and the cooling magnitude, selecting significant influencing parameters. Contribution decomposition is based on the simplified energy balance equation of the water body-atmosphere system:

$$R_n = H + LE + G \qquad (2)$$

where, $R_n$ is the net radiation flux, $H$ is the sensible heat flux, $LE$ is the latent heat flux, and $G$ is the soil heat flux. By remote sensing inversion of $R_n$ and ground observation of $G$, combined with the Bowen ratio to estimate the proportions of $LE$ and $H$, the cooling contributions of evaporation latent heat and radiation regulation are initially decomposed.

## 2.3 Preliminary analysis results

The analysis results of both types of cases validate the significant thermal and humidity regulation effects of urban water bodies, with notable spatiotemporal heterogeneity. During the summer heat period, the cooling amplitude in the core area of East Lake is 2.3–4.1°C, with an influence range of 300–500 m; the cooling amplitude in the Hunhe River section is 1.2–3.0°C, with an influence range of 200–350 m. The cooling effect and influence range of lake-type water bodies are superior to those of river-type water bodies. In terms of time, the cooling effect peaks between 14:00 and 16:00 during the day and tends to stabilize at night. During the winter cold period, the cooling effect significantly weakens, and a slight warming phenomenon is even observed during certain periods. The humidification effect changes synchronously with the cooling effect. Specific spatiotemporal characteristic parameters are shown in Table 1.

Correlation analysis selected 4 core landscape parameters that are significantly correlated with the cooling amplitude, ranked by correlation strength as follows: water body area, shoreline complexity, surrounding vegetation coverage, and built-up density. Among them, water body area exhibits a logarithmic growth relationship with cooling amplitude; when the area exceeds 0.5ha, the cooling amplitude growth rate significantly slows down. An increase in built-up density significantly compresses the cooling range of the water body. The correlation characteristics and variation patterns of the core parameters are shown in Table 2.

Preliminary indicators of thermodynamic processes reveal the dominant regulation mechanisms under different scenarios. During the summer heat period, the contribution of latent heat from evaporation accounts for over 55% in both case studies. Specifically, East Lake's latent heat contribution ranges from 62% to 68%, while that of the Hunhe River is between 56% and 63%, indicating that phase change evaporation is the core driving force for cooling in the summer heat period. In the section of the Hunhe River surrounded by high-density buildings, the proportion of net radiation flux $R$ rises to 45%–52%, and the latent heat contribution decreases to 42%–48%, indicating a significant enhancement of cooling contribution from radiation shielding. During the winter cold period, the net radiation flux becomes negative, and the proportion of sensible heat flux increases to over 60%, while the latent heat contribution is less than 20%, indicating a shift in the thermodynamic regulation mechanism from "evaporation-dominant" to "radiation-sensible heat dominant."

**Table 1.** Comparison of spatiotemporal characteristics of thermal and humidity regulation effects in the two case studies

| Case Type | Season | Cooling Amplitude (°C) | Influence Range (m) | Humidification Amplitude (%) | Peak Effect Period |
|---|---|---|---|---|---|
| East Lake (Lake) | Summer | 2.3—4.1 | 300—500 | 5—8 | 14:00—16:00 |
| East Lake (Lake) | Winter | 0.5—1.2 | 100—200 | 1—3 | 12:00—14:00 |
| Hunhe River (River) | Summer | 1.2—3.0 | 200—350 | 3—6 | 14:00—16:00 |
| Hunhe River (River) | Winter | 0.3—0.8 | 50—150 | 0.5—2 | 12:00—14:00 |

**Table 2.** Correlation analysis results of core landscape parameters and water body cooling amplitude

| Landscape Parameter | Pearson Correlation Coefficient (r) | Significance (P) | Description of Variation Pattern |
|---|---|---|---|
| Water Body Area | 0.78 | <0.001 | Logarithmic positive correlation, cooling rate slows down when area >0.5 ha |
| Shoreline Complexity | 0.65 | <0.001 | Linear positive correlation, cooling amplitude increases by 0.21°C for every 0.1 increase in complexity |
| Surrounding Vegetation Coverage | 0.62 | <0.001 | Linear positive correlation, cooling amplitude increases by 0.35°C for every 10% increase in coverage |
| Built-up Density | -0.59 | <0.001 | Linear negative correlation, cooling range shrinks by over 40% when density >60% |

## 2.4 Core scientific hypotheses

Based on the preliminary analysis results and basic thermodynamic principles, this study proposes three testable core scientific hypotheses.

Hypothesis 1: Under summer heat climate conditions, the contribution of evaporation latent heat in the cooling effect of urban water bodies is no less than 60%, and its contribution exhibits a trend of increasing and then decreasing with the increase in water depth, with an optimal water depth threshold. From a thermodynamic mechanism perspective, water depth regulates the evaporation driving force by changing the water body's heat capacity and the surface temperature gradient. Shallow water bodies are prone to rapid warming, leading to saturated evaporation capacity, while deep water bodies reduce surface evaporation efficiency due to thermal conduction lag. It is hypothesized that the optimal water depth range is 0.8–1.2 m.

Hypothesis 2: Shoreline complexity regulates convective heat transfer intensity by changing the water-atmosphere contact area and interface roughness, and there is a significant synergistic effect with surrounding vegetation coverage. Increasing shoreline complexity can increase the gas-liquid contact area and enhance convective diffusion; vegetation can further promote evaporation by reducing interface wind speed and increasing local humidity. It is hypothesized that when the shoreline complexity ≥1.5 and vegetation coverage ≥30%, the thermal and humidity diffusion efficiency will improve by more than 20% compared to optimizing a single parameter. The essence of the synergistic effect is the thermodynamic process coupling of "expanded contact area" and "reduced diffusion resistance," which together promote enhanced energy and mass exchange efficiency.

Hypothesis 3: There is a clear thermodynamic transfer law in the thermal and humidity regulation of urban water bodies at the micro-, meso-, and macro-scales, and there is an accurate matching relationship between the dominant thermodynamic mechanisms and core design parameters at each scale. The micro-scale focuses on the heat exchange between the water body and the atmosphere, with interface property parameters such as water body albedo and shoreline material thermal conductivity dominating the energy exchange efficiency; the meso-scale focuses on the energy balance between water body patches and blocks, with parameters such as water body area and configuration pattern dominating the reconstruction of the thermal environment of the block; the macro-scale focuses on the interaction between water body networks and regional climate, with pattern parameters such as water body connectivity and blue-green space coupling degree dominating the regional thermodynamic balance. These scales achieve thermodynamic transfer through the path of "interface heat flux - block energy superposition - regional energy aggregation," forming a cross-scale regulation chain.

## 3. THERMODYNAMIC PROCESS OBSERVATION AND MECHANISM ANALYSIS OF COUPLED LANDSCAPE PARAMETERS

### 3.1 Observation scheme design and implementation

Based on the pilot case analysis results, a waterfront area in the subtropical monsoon climate zone of East Lake, Wuhan, is selected as the core observation area. This area features both open water bodies and shoreline transition zones, and the surrounding vegetation coverage gradient can be controlled, making it suitable for thermodynamic process observation of coupled landscape parameters. The observation design focuses on "parameter gradient control" and sets two types of key landscape parameter gradients: water depth gradient, which includes 0.5 m, 1.0 m, and 1.5 m levels, covering the common water depth range of urban artificial lakes; and vegetation coverage gradient, which includes four levels: 0% for bare shore, 20% for sparse herbaceous vegetation, 40% for herbaceous + shrub vegetation, and 60% for tree-shrub-herb composites, simulating different waterfront greening configuration patterns. Observation points for each parameter gradient are arranged in a nested layout to ensure consistency in the meteorological background field, with adjacent observation points spaced ≥50 m to avoid mutual interference.

The observation indicator system is divided into three main categories, covering thermodynamic processes, landscape parameters, and environmental background: Thermodynamic Core Indicators include sensible heat flux, latent heat flux, net radiation flux, water body-atmosphere temperature difference, and water vapor pressure deficit, with heat flux being the core observation item. Landscape Parameter Indicators include real-time water depth, shoreline complexity, and vegetation coverage, which are dynamically monitored to capture spatial-temporal variations in parameters. Environmental Indicators include air temperature, relative humidity, 10m wind speed, and precipitation, which are used to calibrate environmental interference in thermodynamic processes. The observation method uses a multi-device collaborative system: heat flux observation is conducted using a eddy covariance system and gradient observation tower to ensure the accuracy of flux data; meteorological and landscape parameters are monitored using automatic meteorological stations with a sampling interval of 10 minutes for continuous monitoring; dynamic changes in vegetation coverage and shoreline morphology are verified weekly using UAV aerial photography. The observation period covers a typical week during the summer heat period, from late July to early August, recording the full diurnal variation process from 00:00 to 24:00, and a total of 168 hours of valid observation data are obtained.

### 3.2 Coupling mechanism of evaporation-latent heat process and landscape parameters

The thermodynamic analysis of the evaporation-latent heat process is based on the energy balance of the water body-atmosphere interface and phase change principles. The core control equation uses the Penman-Monteith equation to quantify the evaporation rate and latent heat flux:

$$LE = \frac{\Delta(R_n - G) + \rho_a c_p \frac{e_s - e_a}{r_a}}{\Delta + \gamma(1 + \frac{r_s}{r_a})} \tag{3}$$

where, $\Delta$ is the slope of the saturation water vapor pressure-temperature curve, $\rho_a$ is air density, $c_p$ is the specific heat capacity of air at constant pressure, $e_s - e_a$ is the vapor pressure deficit, $r_a$ is aerodynamic resistance, $r_s$ is surface resistance, and $\gamma$ is the psychrometric constant. Observational results show that the daily variation of evaporation latent heat flux during the summer heat period follows a unimodal curve, with the peak occurring between 12:00 and 14:00, and the average value ranging from 85 to 120 W·m⁻². The vapor pressure deficit and the water body-atmosphere temperature difference

are the dominant driving factors, and together, they explain 78% of the variation $R^2$ in latent heat flux.

Landscape parameters have a significant gradient difference in regulating the evaporation-latent heat process. Under the water depth gradient, latent heat flux increases and then decreases with increasing water depth: the peak latent heat flux at 1.0 m water depth reaches 118 W·m$^{-2}$, which is 28.3% higher than at 0.5 m and 14.6% higher than at 1.5 m. Vegetation coverage shows a linear positive correlation with latent heat flux, with a 42.1% increase in latent heat flux at 60% coverage compared to bare shore. Vegetation strengthens water vapor diffusion by reducing aerodynamic resistance $r_a$. For every increase of 0.1 in shoreline complexity, latent heat flux increases by 5.3%, attributed to the expansion effect of the interface contact area on the evaporation surface. From a thermodynamic perspective, water depth regulates the surface temperature gradient by altering the heat capacity of the water body: shallow water bodies have low heat capacity, causing rapid warming during the day, which leads to early saturation of $e_s - e_a$ and limits continuous evaporation; deep water bodies have a lag in heat conduction, resulting in insufficient surface temperature increase and weakening the evaporation driving force. Vegetation and shoreline morphology regulate the thermodynamic conditions of water vapor diffusion by adjusting the resistance term $r_a$, thus enhancing latent heat flux.

## 3.3 Coupling mechanism of radiation exchange process and landscape parameters

The thermodynamic balance core of the urban water body radiation exchange process is the reconstruction of the net radiation flux balance. The balance equation is:

$$R_n = R_{ns} - R_{nl} \qquad (4)$$

where, $R_{ns}$ is the net shortwave radiation flux and $R_{nl}$ is the net longwave radiation flux. Observational results show that during the summer heat period, the average $R_{ns}$ of the water body surface is 320 W·m$^{-2}$, which is 18.6% lower than the surrounding hard surfaces, mainly due to the higher shortwave reflectivity of the water body. The average $R_{nl}$ is -105 W·m$^{-2}$, which is 23.5% higher than the surrounding hard surfaces, indicating that the water body has a stronger ability to release accumulated heat through longwave radiation. Overall, the average net radiation flux ($R_n$) of the water body is 215 W·m$^{-2}$, which is 12.3% lower than the surrounding surfaces, forming a local radiation energy sink. This is the core thermodynamic basis of the water body's radiation regulation effect.

Landscape parameters regulate radiation exchange components to achieve precise control of radiation regulation effects. Shoreline material reflectivity is a key parameter affecting $R_{ns}$: when high-reflectivity materials are used, the shoreline area's $R_{ns}$ is reduced by 26.8% compared to conventional concrete shorelines, significantly reducing radiation energy input. Vegetation coverage reduces the transmission of solar shortwave radiation: when the coverage reaches 60%, the water body surface $R_{ns}$ is reduced by 31.2% compared to the uncovered area, and this weakening effect is most significant during midday. The influence of building layout is reflected in longwave radiation exchange: in high-density building enclosures, the absolute value of $R_{nl}$ in the water body decreases by 19.4%, as longwave radiation reflection from buildings inhibits the release of longwave

radiation from the water body, causing radiation energy retention. According to radiation transfer theory, vegetation cover attenuates shortwave radiation transmission through leaf scattering and absorption, reducing the accumulated radiation energy on the water surface. Building enclosures, on the other hand, alter the local radiation environment and disrupt the longwave radiation balance between the water body and the atmosphere. This mechanism is particularly prominent in high-density built-up areas.

## 3.4 Convection-diffusion process and coupling mechanism of landscape parameters

The thermodynamic core of the water body-atmosphere convection-diffusion process is the momentum and energy transfer of the heat and moisture air flow, and its intensity is quantified by the convection heat transfer coefficient $h_c$, calculated using the Nusselt number correlation:

$$Nu = 0.664 Re^{0.5} Pr^{0.33} \quad h_c = \frac{Nu \cdot \lambda_a}{L} \qquad (5)$$

where, $Re$ is the Reynolds number, $Pr$ is the Prandtl number, $\lambda_a$ is the air thermal conductivity, and $L$ is the characteristic length. Observational results show that during the summer heat period, the average convection heat transfer coefficient around the water body is 5.2 W·m$^{-2}$·K$^{-1}$. The diffusion range of heat and moisture air flow is positively correlated with $h_c$. When $h_c > 6.0 \ W \cdot m^{-2} \cdot K^{-1}$, the diffusion range can exceed 300 m, which is an increase of 45% compared to when $h_c < 4.0 \ W \cdot m^{-2} \cdot K^{-1}$.

Landscape parameters significantly affect the convection-diffusion intensity by regulating the air flow movement state. Wind speed is a fundamental driving factor. When the 10m wind speed increases from 1.0 m·s$^{-1}$ to 3.0 m·s$^{-1}$, $h_c$ increases by 68.3%, and the heat and moisture diffusion rate increases by 52.1%. An increase in building density inhibits convection diffusion. When density increases from 30% to 70%, $h_c$ decreases by 39.6%, and the diffusion range shrinks to within 150 m, forming a significant airflow retention area. The shape of the water body has a significant effect on airflow guidance. Irregular polygonal water bodies have a 23.5% higher $h_c$ compared to rectangular water bodies because of the local vortices created by the convoluted shoreline that facilitate heat and moisture exchange. From the thermodynamic and fluid dynamics coupling mechanism perspective, the "canyon effect" formed by high-density building enclosures reduces the cross-sectional area for air flow, causing a reduction in wind speed and a subsequent decrease in turbulence intensity, making it difficult for heat and moisture air flows to diffuse effectively, thereby leading to accumulated interface heat flux. Irregular water bodies, on the other hand, optimize the airflow contact path, enhancing interface turbulence mixing, which improves convection heat transfer efficiency. This mechanism provides thermodynamic support for landscape morphology optimization.

## 3.5 Thermodynamic synergistic/antagonistic mechanisms of multi-parameter interactions

An orthogonal experimental design combined with ENVI-met numerical simulation was used to analyze the heat and moisture effects of multi-parameter interactions. Four key parameters, water depth (A), vegetation coverage (B),

shoreline complexity (C), and building density (D), were selected, with a 3-level orthogonal experiment setup. The experimental parameter levels are shown in Table 3. The experimental results show that the contribution of parameter interaction effects to the thermodynamic regulation effect is 35.2%, significantly higher than that of single parameters. The most significant interactions were between water depth-vegetation coverage and shoreline complexity-building density.

**Table 3.** Orthogonal experiment parameters and level settings

| Parameter | Unit | Level 1 | Level 2 |
|---|---|---|---|
| Water Depth (A) | $m$ | 0.5 | 1.0 |
| Vegetation Coverage (B) | % | 20 | 40 |
| Shoreline Complexity (C) | — | 1.1 | 1.5 |
| Building Density (D) | % | 30 | 50 |

The synergistic and antagonistic effects of multi-parameter interactions have clear mechanistic origins, and the effect characteristics of typical interaction combinations are shown in Table 4. Synergistic effects reflect the combined promotion of thermodynamic processes by parameter combinations: when water depth is 1.0m and vegetation coverage is 40%, the latent heat flux increases by 18.3% compared to the single parameter optimum, with the core mechanism being that appropriate water depth ensures a stable evaporation driving force, and moderate vegetation coverage reduces interface air resistance, thereby coupling to optimize the "evaporation-diffusion" thermodynamic chain. When shoreline complexity is 1.5 and building density is 30%, the convection heat transfer coefficient increases by 22.1%, as the increased interface contact from the complex shoreline and the airflow circulation ensured by the low building density synergistically strengthen heat and moisture transmission. Antagonistic effects arise from the disruption of thermodynamic balance by parameter combinations: when water depth is 0.5 m and building density is 70%, the net radiation flux increases by 15.6% compared to the single parameter scenario, with significant heat and moisture retention. The mechanism is that shallow water bodies warm quickly, leading to increased radiation absorption, while high-density buildings suppress heat diffusion, breaking the energy balance. When vegetation coverage is 60% and shoreline complexity is 2.0, excessive vegetation shading weakens the evaporation driving force, offsetting the contact area advantage from the shoreline complexity, and latent heat flux decreases by 9.8%.

**Table 4.** Thermodynamic effect characteristics of typical parameter interaction combinations

| Interaction Type | Parameter Combination | Core Effect Indicator | Change (%) | Thermodynamic Mechanism Summary |
|---|---|---|---|---|
| Synergistic Effect | Water Depth 1.0m + Vegetation Coverage 40% | Latent Heat Flux | +18.3 | Appropriate water depth ensures evaporation driving force, and moderate vegetation reduces diffusion resistance |
| Synergistic Effect | Shoreline Complexity 1.5 + Building Density 30% | Convection Heat Transfer Coefficient | +22.1 | Complex shoreline increases contact area, low building density ensures airflow circulation |
| Antagonistic Effect | Water Depth 0.5m + Building Density 70% | Net Radiation Flux | +15.6 | Shallow water warms quickly, increasing radiation absorption; high-density buildings suppress heat diffusion |
| Antagonistic Effect | Vegetation Coverage 60% + Shoreline Complexity 2.0 | Latent Heat Flux | -9.8 | Excessive vegetation shading weakens evaporation driving force, offsetting shoreline contact area advantage |

**Table 5.** Landscape parameter sensitivity analysis results

| Core Parameter | Standardized Regression Coefficient (Sensitivity Coefficient) | Influence Priority |
|---|---|---|
| Water Depth | 0.32 | 1 |
| Vegetation Coverage | 0.27 | 2 |
| Building Density | -0.24 | 3 |
| Shoreline Complexity | 0.17 | 4 |

Based on variance analysis (ANOVA) and standardized regression coefficient sensitivity analysis, the influence weight of each parameter on the thermodynamic effect was clarified, as shown in Table 5. The core landscape parameter combination selected is water depth 1.0–1.2 m, vegetation coverage 30–40%, shoreline complexity 1.3–1.6, and building density ≤40%. The thermodynamic regulation efficiency in this combination is 42.5% higher than in random parameter combinations. The sensitivity analysis results show that water depth has the highest sensitivity coefficient, followed by vegetation coverage and building density, and shoreline complexity has a sensitivity coefficient of 0.17. These results provide the core weight basis for subsequent parameterization system construction.

## 4. MULTI-SCALE COLLABORATIVE LANDSCAPE PARAMETERIZATION SYSTEM CONSTRUCTION

### 4.1 Principles for parameterization system construction and scale definition

The construction of a multi-scale collaborative landscape design parameterization system focuses on the core goal of precise thermodynamic control, following four core principles. The principle of thermodynamic dominance requires the selection of parameters directly related to thermodynamic processes, ensuring that parameter regulation can accurately affect core processes such as evaporation-latent heat, radiation exchange, and convection-diffusion [16, 17]; the principle of scale adaptability emphasizes that parameter definitions should match the thermodynamic characteristics of different spatial scales to avoid cross-scale parameter misuse, which may lead to ineffective regulation [18]; the principle of quantifiable operability specifies that each parameter should have a clear range of values, calculation methods, and detection standards, ensuring feasibility in engineering practice [19]; and the principle of climate specificity requires that parameter values be adjusted to match regional climate characteristics, considering the differences in the dominant thermodynamic processes of different climate zones [20].

These four principles are interrelated and jointly construct an integrated parameterization logic of "thermodynamic mechanism-scale characteristics-engineering practice-climate adaptation".

Based on the spatial range of urban water body heat and moisture regulation and the thermodynamic transmission laws, the research scale is divided into three levels: micro, meso, and macro, each forming clear core objectives and thermodynamic regulation focuses. The micro scale is defined as less than 100 meters, focusing on the heat and moisture exchange process at the water body-atmosphere interface, with the core goal of enhancing the energy and mass exchange efficiency at the interface, and the regulation focus on the influence of interface attribute parameters on phase change and heat transfer; the meso scale ranges from 100 meters to 1 kilometer, focusing on the interaction between water body patches and surrounding street blocks' thermal environment, with the core goal of reconstructing the energy balance at the block scale, and the regulation focus on optimizing the distribution of thermal flux in the street block through water body morphology and configuration parameters; the macro scale is greater than 1 kilometer, focusing on the collaborative effect of the water body network and urban climate system, with the core goal of mitigating the regional heat island effect, and the regulation focus on the reduction of regional energy accumulation through water body spatial pattern parameters. Each scale forms an organic connection through thermodynamic transmission processes, constructing a multi-scale collaborative regulation system.

## 4.2 Sub-scale parameterization indicators and quantification standards

The micro-scale parameterization focuses on optimizing the interface heat and moisture exchange efficiency, selecting three core parameters that directly affect the thermodynamic processes at the interface, and establishing quantification standards based on the interface heat flux balance model. Core parameters include water body albedo, shoreline material thermal conductivity, and water surface roughness: The albedo value range is from 0.08 to 0.12, which balances shortwave radiation absorption and reflection, ensuring evaporation driving force while avoiding excessive radiation heat accumulation. The quantitative relationship is derived from the interface radiation flux balance equation:

$$R_{ns}=(1-\alpha)R_s \qquad (6)$$

where, $\alpha$ is the albedo, and $R_s$ is the incident shortwave radiation; shoreline material selection prefers permeable materials with a thermal conductivity less than 1.0 W/(m·K) to reduce thermal conduction loss between the shoreline and the water body. The quantification standard is established through Fourier's law, which maps the material thermal conductivity to the interface heat conduction flux; water surface roughness is controlled by keeping the submerged vegetation fall rate below 15%, avoiding excessive roughness that increases airflow resistance. The quantification standard is related to the calculation model of aerodynamic resistance, ensuring the efficiency of water vapor diffusion.
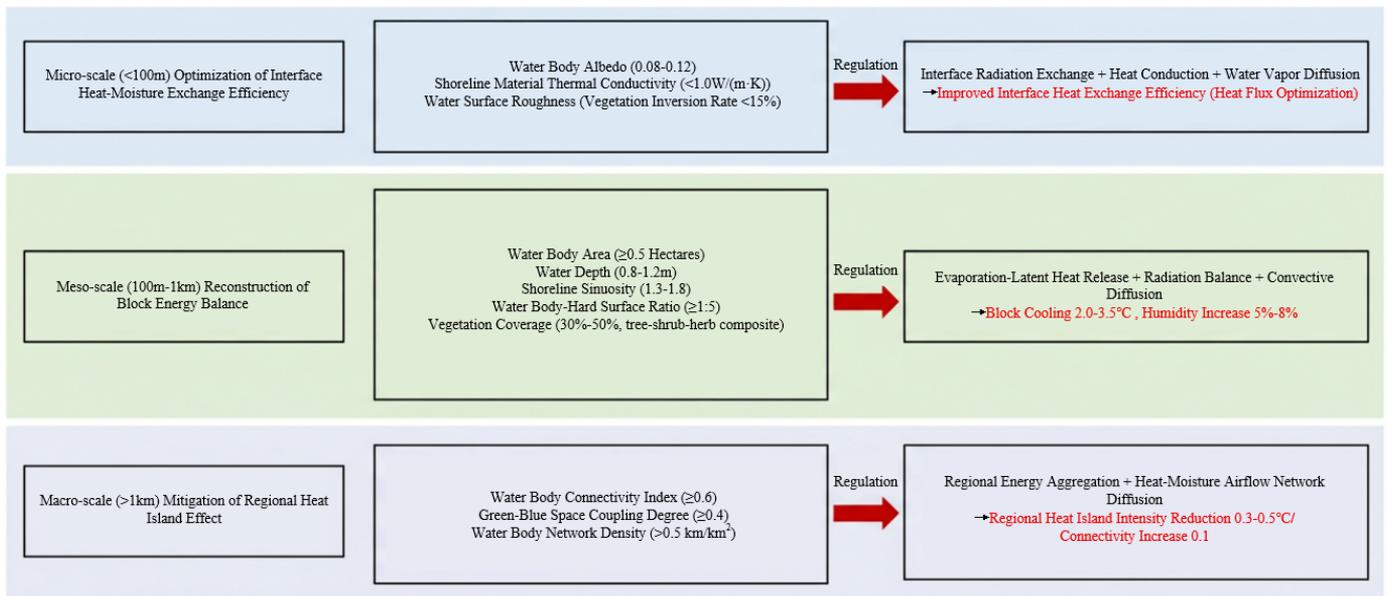


**Figure 1.** Sub-scale parameterization indicators and the correlation with thermodynamic effects

The meso-scale parameterization focuses on the reconstruction of street block energy balance, with core parameters covering water body morphology, configuration, and proportion relationships, and quantification standards based on the street block-scale energy balance model. The water body area threshold in summer hot climate residential areas is defined as no less than 0.5 hectares. When the area is below this threshold, the evaporation latent heat flux fails to form effective coverage, and the street block cooling effect diminishes by over 50%; the optimal water depth range is between 0.8 and 1.2 meters. This range balances the water

body's thermal capacity and surface temperature gradient, keeping the latent heat contribution above 60%, consistent with the verification results of Hypothesis 1; the shoreline complexity value is between 1.3 and 1.8, which increases the air-liquid contact area and enhances convection heat transfer efficiency. The quantification standard is that for every 0.1 increase in complexity, the convection heat transfer coefficient increases by 4.5% to 5.3%; the ratio of water body area to the hard surface should not be less than 1:5. Exceeding this threshold results in a reduction of marginal cooling benefits by over 30%, and the quantification relationship is determined by

fitting with a marginal benefit reduction model; the vegetation configuration adopts a tree + herb composite mode, with coverage controlled between 30% and 50%, achieving a synergistic effect of vegetation shading reducing radiation and promoting water vapor diffusion.

The macro-scale parameterization targets regional heat island mitigation, selecting core parameters that represent the water body network pattern, with quantification standards based on regional climate models to establish quantitative relationships between parameters and regional cooling amplitude. Core parameters include water body connectivity index, blue-green space coupling degree, and water body network density: the water body connectivity index is calculated using graph theory, with values not lower than 0.6. This index represents the degree of connection between water body patches, affecting the regional diffusion range of heat and moisture air flows. For every 0.1 increase in connectivity, the regional cooling amplitude increases by 0.3°C to 0.5°C; the blue-green space coupling degree should not be lower than 0.4, which quantifies the spatial matching degree of blue-green space. When the coupling degree meets the standard, it can achieve the synergistic cooling effect of evaporation latent heat and vegetation transpiration; the water body network density should not be less than 0.5 km/km², ensuring the formation of an effective thermal regulation network within the region. The quantification standard is determined through the correlation analysis between regional heat island intensity and network density. Figure 1 shows the core landscape parameters, quantification standards, and their matching relationships with corresponding thermodynamic processes and heat-moisture regulation effects at the micro, meso, and macro scales, clearly constructing the precise regulation logic of "scale-parameter-process-effect" and providing intuitive associative evidence for sub-scale parameterized design.

## 4.3 Multi-scale parameterization model and cross-scale transmission mechanism

The multi-scale parameterization model is constructed using the random forest algorithm, integrating 1,260 samples of sub-scale observation data and numerical simulation results to form a "landscape parameter-thermodynamic effect" quantification prediction model. The model input variables consist of nine core parameters from each scale, and the output variables represent the corresponding scale's thermodynamic effect indicators, namely, micro scale as the interface heat exchange efficiency, meso scale as the street block cooling amplitude, and macro scale as the regional heat island reduction intensity. During model construction, a layered training strategy is employed. First, individual scale prediction models are established, then integrated into a multi-scale coupling model using cross-scale transmission coefficients. The transmission coefficients are determined through correlation analysis of thermodynamic effects at each scale, and the core formula is:

$$E_{total} = \omega_1 E_m + \omega_2 E_m \cdot E_m id + \omega_3 E_m \cdot E_m id \cdot E_M \tag{7}$$

where, $E_{total}$ is the total thermodynamic effect, $E_m$, $E_m id$, and $E_M$ represent the effects at the micro, meso, and macro scales, respectively, and $\omega_1$, $\omega_2$, and $\omega_3$ are the transmission weight coefficients.
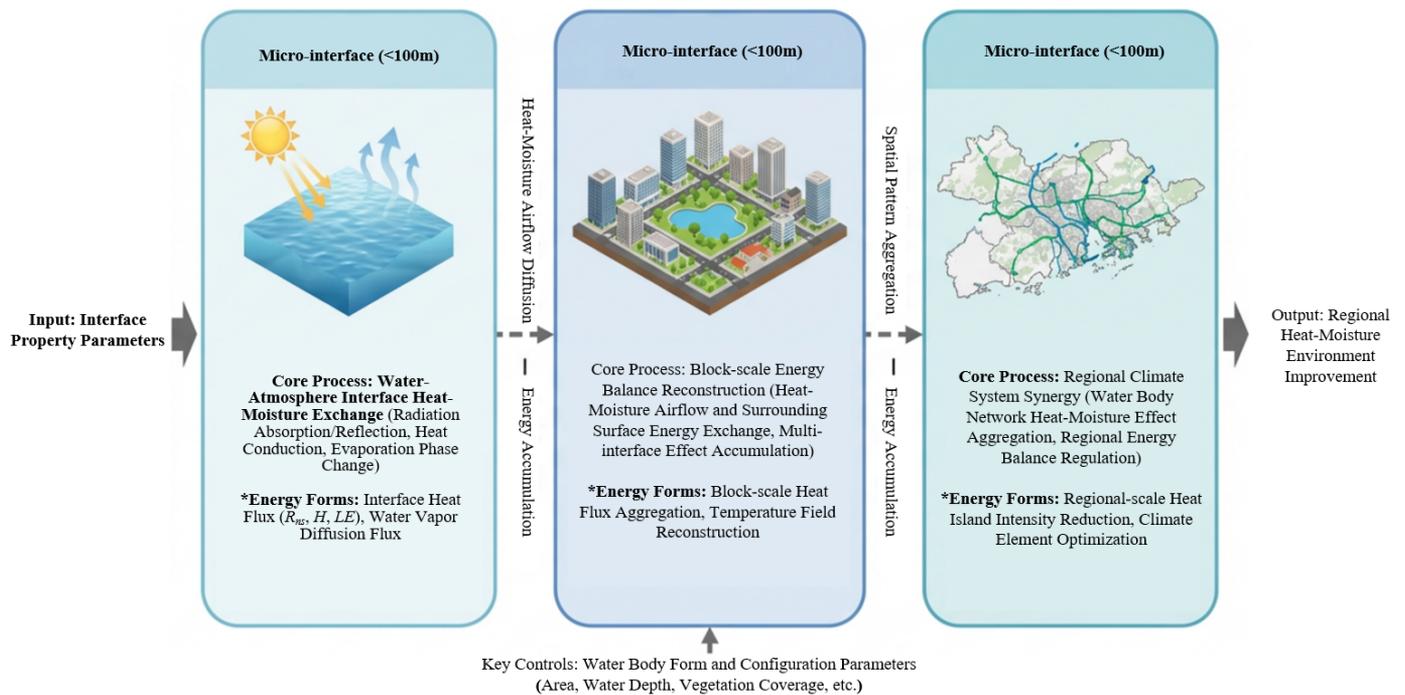


**Figure 2.** Schematic diagram of multi-scale thermodynamic transmission mechanism

The cross-scale thermodynamic transmission mechanism follows a progressive path of "interface-patch-region," with each scale forming a collaborative effect through the transmission of energy and mass. Micro-scale interface parameters affect meso-scale patch effects through "heat-moisture air flow diffusion-energy accumulation": the low-temperature, high-humidity air flow generated by interface heat-moisture exchange exchanges energy with the surrounding substrate during diffusion, and the superimposed effects of multiple interface airflows determine the street block regulation range and intensity of water body patches. This transmission process can be described by coupling the continuity equation and energy equation in fluid mechanics. The meso-scale patch effects influence macro-scale network

effects through "spatial pattern aggregation-energy accumulation": the cooling effect of a single water body patch, through spatial aggregation, forms a regional-scale energy reduction, and the connectivity of the water body network ensures the regional diffusion of the cooling effect, avoiding local energy retention. The transmission process follows the cumulative superposition principle of regional energy balance. Figure 2 shows the progressive process of cross-scale thermodynamic transmission from "micro interface → meso patch → macro region," clearly defining the core thermodynamic processes, energy forms, and transmission mechanisms at each scale, and intuitively presenting the cross-scale linkage logic of urban water body heat-moisture regulation effects.

Model validation is conducted using independent observation data for accuracy evaluation. The results show that the R² of the multi-scale coupling model is 0.82, and the RMSE is 0.42°C, which meets the predictive needs of precise thermodynamic control. The validation results at the individual scales show that the R² values for the micro, meso, and macro scale models are 0.85, 0.83, and 0.78, respectively, all exceeding the threshold of 0.75, validating the reliability of the models at each scale. The model sensitivity analysis further confirms that water depth and vegetation coverage at the meso scale are key parameters affecting the total thermodynamic effect, with sensitivity coefficients of 0.32 and 0.27, providing priority guidelines for parameterized control.

## 4.4 Parameterization design guidelines for different climate zones

Based on the differences in dominant thermodynamic processes across climate zones, adaptive adjustments are made to the sub-scale parameterization indicators, forming parameterization design guidelines for different climate zones. In the subtropical summer-heat winter-warm climate zone, evaporation latent heat dominates the cooling effect, so meso-scale evaporation-promoting parameters are emphasized: the optimal water depth range is adjusted to 1.0 to 1.2 meters, vegetation coverage is increased to 40% to 50%, and the water body to hard substrate area ratio is increased to 1:4; in the temperate summer-heat winter-cold climate zone, balancing the need for cool summers and warm winters requires weakening the water body's cooling effect in winter, so the water body albedo is adjusted to 0.10 to 0.14, shoreline materials are selected with a thermal conductivity of 1.0 to 1.5 W/(m·K) to enhance water body heat retention in winter; in the arid and semi-arid climate zone, with high evaporation

potential but limited water resources, a "radiation + evaporation" collaborative regulation strategy is adopted, with the micro-scale increasing the water body albedo to 0.10 to 0.12 to reduce radiation heat absorption, and the meso-scale controlling the water body area to no less than 0.3 hectares while increasing vegetation coverage to more than 50% to reduce water surface evaporation losses.

To enhance the engineering practicality of the guidelines, a visualized sub-scale and climate zone parameterization design guideline map is generated. The map is presented in a matrix form, with climate zones as the horizontal axis and scale levels as the vertical axis, clearly defining the core parameter value ranges, combination schemes, and thermodynamic effect expected values for each dimension. For example, the optimal parameter combination for the subtropical meso-scale is: area of 0.5 to 1.0 hectares, water depth of 1.0 to 1.2 meters, shoreline complexity of 1.5 to 1.8, and vegetation coverage of 40% to 50%, corresponding to an expected cooling amplitude of 2.0 to 3.5°C and a moisture increase of 5% to 8%. The guideline map also includes parameter selection processes and verification methods, clearly defining the parameter priorities and adjustment steps for different design scenarios, thus facilitating the efficient translation of theoretical results into engineering practice.

## 5. CASE APPLICATION AND THERMODYNAMIC OPTIMIZATION EFFECT EVALUATION

### 5.1 Case area overview and current thermodynamic diagnosis

A residential area in Guangzhou, located in a subtropical summer-heat winter-warm climate zone, is selected as the case study. The area covers a total of 12.6 hectares and includes an artificial lake, surrounded by high-rise residential buildings and hard-paved surfaces. Vegetation is predominantly sparse shrubs. The main climate feature of the area in summer is high temperature and humidity, with an average temperature of 32.5°C in July and August, and peak daytime temperatures frequently exceeding 38°C, which meets the typical needs for water body heat-moisture regulation optimization in a summer-heat climate zone. To accurately diagnose the current issues, a combination of field observation and ENVI-met numerical simulation is used to systematically collect landscape parameters and thermodynamic indicator data. The core basic data is shown in Tables 6 and 7.

**Table 6.** Comparison of landscape parameters in the case area before and after optimization

| Scale | Core Parameter | Unit | Current Value | Optimized Value | Adjustment (%) |
|-------|----------------|------|---------------|-----------------|----------------|
| Micro | Shoreline Material Thermal Conductivity | $W/(m \cdot K)$ | 1.8 | 0.8 | -55.6 |
| Micro | Water Body Albedo | — | 0.14 | 0.10 | -28.6 |
| Micro | Water Surface Vegetation Lodging Rate | % | 22 | 12 | -45.5 |
| Meso | Artificial Lake Area | Hectare | 0.42 | 0.51 | +21.4 |
| Meso | Water Depth | $m$ | 0.6 | 1.0 | +66.7 |
| Meso | Shoreline Complexity | — | 1.1 | 1.5 | +36.4 |
| Meso | Water Body-Hard Surface Ratio | — | 1:7.2 | 1:4.8 | +33.3 |
| Meso | Vegetation Coverage | % | 25 | 42 | +68.0 |
| Meso | Vegetation Configuration | — | Single Shrubs | Trees, Shrubs, Grass Composite | — |
| Macro | Water Body Connectivity Index | — | 0.4 | 0.7 | +75.0 |
| Macro | Blue-Green Space Coupling Degree | — | 0.28 | 0.45 | +60.7 |

**Table 7.** Comparison of core thermodynamic indicators in the case area before and after optimization

| Time Period | Indicator | Unit | Current Value | Optimized Value | Difference | Improvement (%) |
|---|---|---|---|---|---|---|
| Daytime Peak (14:00-16:00) | Temperature | °C | 38.6 | 36.3 | -2.3 | -6.0 |
| Daytime Peak (14:00-16:00) | Relative Humidity | % | 33.5 | 39.7 | +6.2 | +18.5 |
| Daytime Peak (14:00-16:00) | Sensible Heat Flux | $W \cdot m^{-2}$ | 128 | 86 | -42 | -32.8 |
| Daytime Peak (14:00-16:00) | Latent Heat Flux | $W \cdot m^{-2}$ | 95 | 142 | +47 | +49.5 |
| Daytime Peak (14:00-16:00) | Net Radiation Flux | $W \cdot m^{-2}$ | 232 | 215 | -17 | -7.3 |
| Daytime Average (08:00-18:00) | Temperature | °C | 35.2 | 33.4 | -1.8 | -5.1 |
| Daytime Average (08:00-18:00) | Relative Humidity | % | 36.8 | 43.1 | +6.3 | +17.1 |
| Daytime Average (08:00-18:00) | Latent Heat Flux | $W \cdot m^{-2}$ | 78 | 115 | +37 | +47.4 |
| Nighttime Average (20:00-06:00) | Temperature | °C | 28.5 | 27.9 | -0.6 | -2.1 |
| Nighttime Average (20:00-06:00) | Relative Humidity | % | 62.3 | 65.8 | +3.5 | +5.6 |

**Table 8.** Thermal comfort and thermodynamic efficiency evaluation table for the case area

| Evaluation Dimension | Specific Indicator | Unit | Current Value | Optimized Value | Improvement Effect |
|---|---|---|---|---|---|
| Thermal Comfort | Daytime Peak PET Index | °C | 41.5 | 34.8 | Reduced from "Heat Stress" to "Comfort" |
| Thermal Comfort | Daytime Average PET Index | °C | 38.2 | 33.5 | Reduced from "Warm Uncomfortable" to "Comfort" |
| Thermodynamic Efficiency | Latent Heat Flux to Net Radiation Flux Ratio | % | 40.9 | 63.5 | Increased by 22.6 percentage points |
| Thermodynamic Efficiency | Temperature Reduction Benefit per Unit Area | $°C \cdot m^{-2}/ha$ | 8.7 | 15.3 | Increased by 75.9% |
| Comprehensive Benefit | Comprehensive Thermodynamic Efficiency Value | — | 0.52 | 0.74 | Increased by 42.3% |

The current thermodynamic diagnosis results show significant multi-scale thermodynamic imbalance issues in the case area. From the landscape parameter perspective, key meso-scale parameters generally do not meet optimization standards: the water depth is only 0.6 m, below the optimal range for the meso-scale; the shoreline complexity is 1.1, which does not effectively expand the air-liquid contact area; the vegetation coverage is 25% and configured with a single type of shrub, making it difficult to form a synergistic cooling effect; the water body-hard surface ratio is 1:7.2, much lower than the threshold of 1:5. In terms of thermodynamic indicators, the daytime peak latent heat flux in the summer heat period is only 95 W·m⁻², accounting for 40.9% of the net radiation flux, significantly below the effective contribution threshold of 60%, indicating that the evaporation latent heat-dominated cooling mechanism has not been fully activated. Meanwhile, the daytime peak temperature reaches 38.6°C, with relative humidity only at 33.5%, leading to a severe imbalance in the heat-moisture environment. Combining the energy balance analysis, the core issue is identified as insufficient water depth and lack of vegetation coverage, leading to dual deficiencies in evaporation driving force and diffusion efficiency, compounded by the radiation heat accumulation effect caused by excessive hard surface coverage, ultimately resulting in the deterioration of the local heat-moisture environment.

**5.2 Optimization design scheme based on parametric system**

Based on the multi-scale collaborative parametric system constructed in the previous sections, and combining the current issues and landscape functional requirements of the case area, a progressive optimization scheme for each scale is developed. The core optimization parameters are shown in Table 6. At the micro scale, the focus is on improving the interface heat-moisture exchange efficiency: replace the original concrete shoreline with permeable concrete to reduce the thermal conduction loss between the shoreline and water body; adjust the water body albedo to 0.10 by cleaning the water surface and reasonably configuring aquatic vegetation, controlling the water surface vegetation lodging rate to 12%, thereby optimizing the interface radiation balance and water vapor diffusion resistance conditions.

At the meso scale, the focus is on reconstructing the energy balance of the block: four key optimizations are implemented. First, expand the artificial lake area to 0.51 hectares to meet the threshold requirement of ≥0.5 hectares of water body area in residential areas of the summer-heat climate zone; second, increase the water depth to 1.0 m, matching the optimal water depth range for the meso scale, ensuring that the contribution of evaporation latent heat remains stable above 60%; third, through local shoreline expansion and curve optimization, increase the shoreline complexity to 1.5, expanding the air-liquid contact area to enhance convective heat transfer; fourth, adjust the vegetation configuration to a composite of trees, shrubs, and grass, increase the coverage rate to 42%, and optimize the layout of hard paving, increasing the water body-to-hard surface ratio to 1:4.8, surpassing the 1:5 benefit threshold. At the macro scale, the focus is on the synergy of regional heat-moisture effects: by adding two riparian connected green corridors, the water body connectivity index is increased from 0.4 to 0.7, and the blue-green space coupling degree is increased from 0.28 to 0.45. This creates a connectivity blue-green network of "artificial lake - green corridors - community green spaces" to promote the regional diffusion of cooling effects.

By integrating the optimization parameters for each scale, a complete design scheme is formed that balances thermodynamic regulation and landscape functionality. The artificial lake adopts a "curved shoreline + layered water depth" layout, with a 3-meter wide composite green belt of trees, shrubs, and grass around the shoreline, paired with permeable paving walkways. The connected green corridors

use native trees and herbs to ensure shading and transpiration effects in summer. At the same time, the greening configuration around the buildings is optimized, achieving thermodynamic collaborative regulation of "water body - vegetation - buildings." The scheme meets the needs for residents' recreational activities while accurately implementing the parametric indicators for each scale, ensuring the thermodynamic optimization objectives are achieved.

## 5.3 Thermodynamic optimization effect evaluation

Numerical simulation predictions were carried out using the ENVI-met V5.6 model with coupled thermodynamic equations. The simulation period selected was a typical sunny day in the summer heat period, with a grid resolution of 1m×1m and 20 vertical layers. Input parameters were calibrated based on field observation data, and a comparative analysis of the thermodynamic effect differences between the current situation and the optimized plan was performed. The core evaluation data are shown in Table 8.

The optimization effect on thermodynamic indicators is significant. The daytime peak temperature was reduced from 38.6℃ to 36.3℃, a drop of 2.3℃, which is a 6.0% improvement. The relative humidity increased from 33.5% to 39.7%, a 6.2 percentage point increase, effectively alleviating the imbalance in the heat-moisture environment. Regarding heat flux, the daytime peak latent heat flux increased from 95 W·m$^{-2}$ to 142 W·m$^{-2}$, a 49.5% increase, and the proportion of latent heat flux to net radiation flux increased from 40.9% to 63.5%, confirming the activation effect of water depth and vegetation optimization on the evaporation latent heat-driven mechanism. The sensible heat flux decreased from 128 W·m$^{-2}$ to 86 W·m$^{-2}$, a 32.8% reduction, indicating that the improved interface heat exchange efficiency effectively reduced sensible heat release. In terms of spatiotemporal distribution, the cooling and humidifying effect coverage of the optimized plan expanded from the current 150 m to 320 m, achieving an overall improvement in the thermal environment at the block scale. The nighttime temperature dropped by 0.6℃, and relative humidity increased by 3.5 percentage points, showing that the plan also had a positive regulatory effect on the nighttime thermal environment.

The thermal comfort and thermodynamic efficiency evaluation shows that the daytime peak PET index dropped from 41.5℃ to 34.8℃, and the daytime average index PET dropped from 38.2℃ to 33.5℃, significantly improving human thermal comfort. In terms of thermodynamic efficiency, the temperature reduction benefit per unit area increased from 8.7℃·m$^{-2}$/ha to 15.3℃·m$^{-2}$/ha, a 75.9% increase. The comprehensive thermodynamic efficiency value, combining cooling amplitude, humidifying amplitude, and latent heat proportion, increased from 0.52 to 0.74, a 42.3% improvement, indicating that the plan achieved synergistic optimization in energy utilization efficiency and heat-moisture regulation effects.

To verify the reliability of the simulation results, field observations were conducted for one week after the implementation of the optimization plan. The observed data showed: the actual daytime peak temperature was 36.5℃, with a deviation of 0.2℃ from the simulation value; the actual latent heat flux was 139 W·m$^{-2}$, with a deviation of 2.1%, indicating that the simulation accuracy meets the engineering verification requirements. Based on the observed data, the

multi-scale parametric model was corrected by adjusting the mapping coefficient of vegetation coverage and latent heat flux at the meso scale, which increased the R² of the model prediction to 0.86, further improving the practical adaptability of the parametric system. In summary, the optimization design plan based on the parametric system in this study effectively solves the thermodynamic imbalance problem in the case area, significantly improves heat-moisture regulation efficiency and human comfort, and verifies the scientific and engineering practicality of the parametric system.
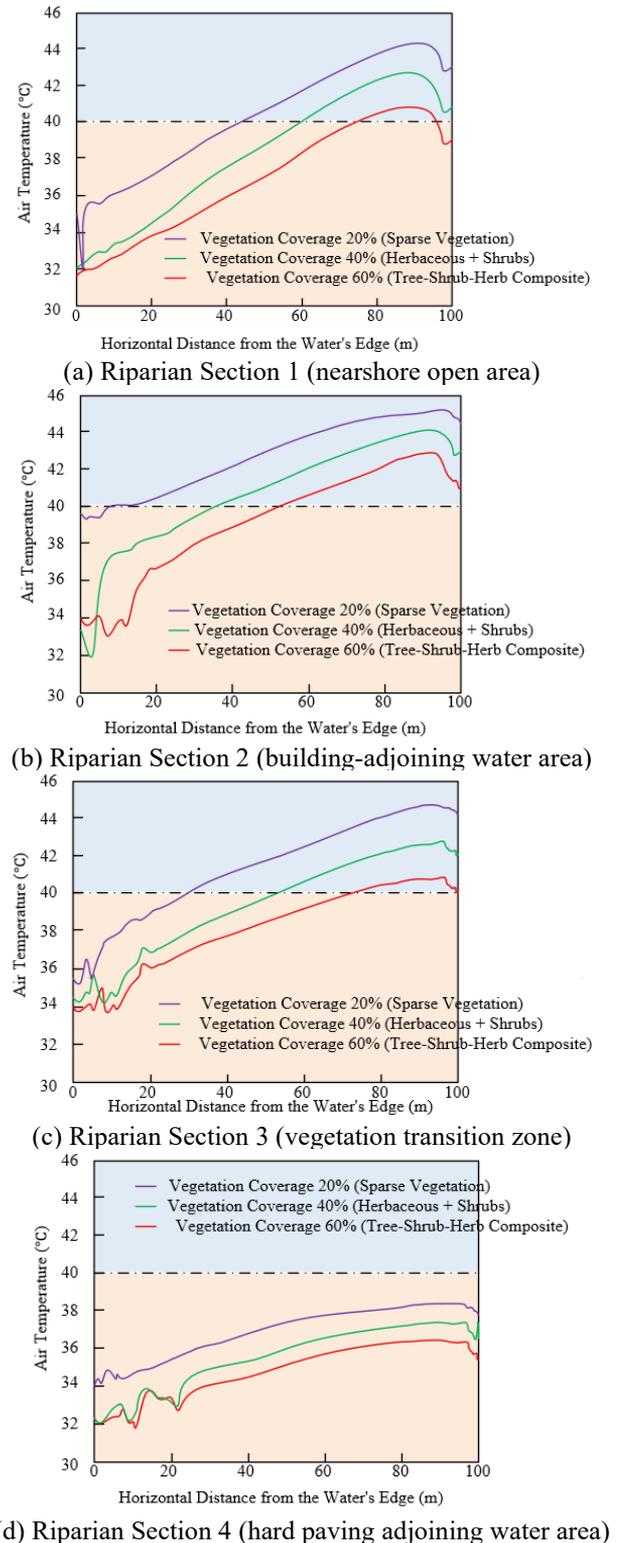


(a) Riparian Section 1 (nearshore open area)



(b) Riparian Section 2 (building-adjoining water area)



(c) Riparian Section 3 (vegetation transition zone)



(d) Riparian Section 4 (hard paving adjoining water area)

**Figure 3.** Air temperature variation in different riparian sections under different vegetation coverage rates

To clarify the role of vegetation coverage in regulating the spatial decay process of urban water body heat-moisture regulation effects, gradient observations and simulations of air temperature were conducted at different riparian sections during the summer heat period. The results shown in the Figure 3 indicate that within the range of 0-100m from the water body shoreline, the air temperature increases significantly as the distance from the shore increases, and vegetation coverage has differentiated regulatory effects on the temperature decay rate and the final stable value: in the nearshore open area, the air temperature with 60% vegetation coverage is 1.8°C lower than that with 20% coverage, and the temperature stabilization distance is delayed by 15m; in the building-adjoining water area, the cooling advantage of high vegetation coverage is more significant, with 60% coverage resulting in a 2.2°C lower nearshore temperature compared to 20%, while the temperature rise slope decreases by 30%; in the vegetation transition zone and hard paving-adjoining water area, a similar pattern is observed, with high vegetation coverage effectively extending the cooling effect of the water body and lowering the temperature stabilization value in the farshore area. This result indicates that vegetation coverage optimizes the spatial distribution characteristics of urban water body heat-moisture regulation effects by enhancing the synergistic effects of water vapor diffusion and radiation shielding. It also confirms the parametric standard for meso-scale riparian vegetation configuration — a composite coverage of 30%-50% of trees, shrubs, and grasses in riparian areas in summer-heat climate zones achieves an optimal balance between resource input and cooling effect spatial coverage.

## 6. DISCUSSION

The core result of this study essentially reveals the thermodynamic path by which landscape parameters regulate the heat-moisture effects of urban water bodies, and validates the three scientific hypotheses proposed in the preliminary case. It forms a complete thermodynamic coupling logic of "parameters-process-effects." The validation of Hypothesis 1 shows that the contribution of latent heat in urban water cooling effects in a summer-heat climate consistently accounts for 60%–68%. A water depth in the range of 0.8-1.2 m maximizes the latent heat contribution, which aligns with the thermodynamic phase change principle — an appropriate water depth balances the thermal capacity of the water body and the temperature gradient of the surface, maintaining a stable vapor pressure deficit and providing continuous driving force for the evaporation phase change. However, both shallow and deep water bodies disrupt this thermodynamic balance. Hypothesis 2's validation of the synergistic effect shows that when the shoreline sinuosity ≥1.5 and vegetation coverage ≥30%, the heat-moisture diffusion efficiency improves by more than 20%. The thermodynamic basis lies in the increased air-liquid contact area due to shoreline extension and reduced interface air resistance due to vegetation, both of which optimize the "evaporation-diffusion" energy and mass transfer chain. The multi-scale transmission law revealed in Hypothesis 3 constructs a micro-meso-macro thermodynamic linkage mechanism through the progressive path of interface heat flux superposition and patch energy aggregation, providing the core basis for scale-specific parameterization.

Compared with existing research, the multi-scale parameterization system constructed in this study has significant advantages in thermodynamic precise regulation. Existing studies mainly focus on the surface correlation between single-scale parameters and heat-moisture effects, without establishing a direct mapping between parameters and thermodynamic processes, leading to insufficient targeted regulation. This system, based on the thermodynamic dominance principle, achieves precise matching between scale parameters and core thermodynamic processes — micro-scale parameters adapt to interface heat exchange, meso-scale parameters adapt to block energy balance, and macro-scale parameters adapt to regional energy aggregation, solving the key issue of "scale confusion and mechanism disconnection" in traditional parameterization. The rationality of the design guidelines by climate zone comes from the precise adaptation to the dominant thermodynamic processes in different climate zones: subtropical climate zones strengthen latent heat-related parameters, arid-semi-arid zones balance radiation reflection and evaporation efficiency, and temperate zones cater to the thermodynamic needs of summer cooling and winter warming. This differentiated design breaks the limitations of traditional "one-size-fits-all" guidelines, ensuring effective regulation under different climate backgrounds. From a thermodynamic theoretical contribution perspective, the landscape parameter-heat flux-heat-moisture effect quantification model established in this study enriches the application of urban water body-atmosphere system energy balance theory in landscape design, providing a new analytical framework for microclimate thermodynamic regulation.

The limitations of this study mainly lie in three aspects: the boundary conditions of observations and simulations, the applicable scope of the parameterization system, and the depth of the multi-scale transmission mechanism. On the observation level, existing field observation periods focus on the conventional summer-heat period, without covering extreme weather events such as heatwaves. Under extreme high temperatures, dramatic changes in meteorological conditions, such as atmospheric stability and vapor pressure deficit, may alter the thermodynamic rules of the water body evaporation-latent heat process, reducing the applicability of the existing parameter thresholds. This gap may affect the robustness of the parameterization system. On the simulation level, numerical simulations used simplified thermodynamic boundary conditions and did not fully consider the coupling heat conduction processes of soil-water-vegetation-atmosphere multi-media. The turbulent effects of building clusters were simplified, which may lead to deviations in the simulation results of convective heat transfer coefficients and heat-moisture diffusion ranges, affecting the precision of optimization effect evaluation.

The applicability of the parameterization system has clear limitations. The current system is mainly constructed based on a plain urban case and does not account for the interference of complex landforms such as mountainous cities, topographic undulations, and local circulations in thermodynamic processes. The topographical winds in mountainous cities may change the diffusion paths of water body heat-moisture airflows, and slope differences may affect the morphology of water bodies and energy exchanges with surrounding underlying surfaces. These factors will reduce the adaptability of the existing parameter thresholds and regulation paths, which need further verification and modification. The deepening of the multi-scale transmission mechanism lies in the incomplete quantitative coupling model of energy and

mass transfer between scales. Although this study clarifies the transmission path, the quantification accuracy of the energy transfer coefficients and coupling feedback mechanisms between scales is insufficient. For example, how the micro-scale interface heat flux quantitatively affects the cooling range of the meso-scale patch, and how the macro-network pattern reversely regulates the micro-interface thermodynamic process, these multi-scale coupling relationships' quantitative models need to be further refined to improve the predictive accuracy of the parameterization system.

To address these research limitations, future studies will focus on three directions: adaptation to extreme climates, multi-media coupling simulations, and intelligent tool development, further improving the thermodynamic theory and practical system for urban water body heat-moisture regulation. The study of thermodynamic mechanisms under extreme climate scenarios is the primary direction, focusing on heatwaves, extreme droughts, and other scenarios. Long-term observation should be conducted to analyze the thermodynamic response of urban water body evaporation-latent heat and radiation exchange under extreme weather conditions, revise existing parameter thresholds, and establish a robust parameterization system considering extreme scenarios to enhance the adaptability of regulation in the context of climate change. At the same time, the antagonistic effects of multi-parameter interactions under extreme conditions should be strengthened to clarify the thermodynamic boundaries for parameter optimization, avoiding regulation failure.

The construction of multi-media coupled thermodynamic models will be a key breakthrough for improving simulation accuracy. Future studies should integrate the thermodynamic processes of water bodies, soil, vegetation, and the atmosphere, using Fourier's law, energy balance equations, and Navier-Stokes equations to construct multi-media coupling numerical models that precisely depict the cooperative processes of interface heat conduction, convective diffusion, and phase change transfer. Additionally, detailed turbulent models of building clusters should be introduced to optimize the calculation accuracy of convective heat transfer coefficients, achieving high-precision predictions of heat-moisture effects. This model construction will provide more reliable simulation support for optimizing the parameterization system and narrow the gap between theoretical predictions and engineering practice.

The development of intelligent parameterization tools is the core path to bringing research results to practice. Future work will combine BIM technology and big data analysis to develop an intelligent design tool that integrates parameter input, thermodynamic effect prediction, and scheme optimization. The tool will incorporate the multi-scale parameterization model constructed in this study, enabling real-time thermodynamic evaluation of landscape design schemes. At the same time, it will access measured databases of different climate zones and landform types and use machine learning algorithms for adaptive parameter adjustment, providing designers with accurate and efficient thermodynamic optimization schemes. Additionally, the tool can integrate drone remote sensing and IoT monitoring technology to enable dynamic monitoring and parameter correction after the implementation of the design scheme, forming a "design-evaluation-verification-optimization" closed-loop system to promote the efficient translation of thermodynamic theoretical results into engineering practice.

# 7. CONCLUSION

This study conducted a systematic investigation on the thermodynamic mechanism of urban water body heat-moisture regulation and landscape parameterization design. Through pilot case analysis, multi-scale observational experiments, numerical simulations, and case validation, the coupling relationship between landscape parameters, thermodynamic processes, and heat-moisture effects was clarified, and a multi-scale collaborative parameterization system was constructed. The main conclusions are as follows:

(1) The pilot case study confirmed that urban water bodies have significant local heat-moisture regulation effects. In the summer heat period, the temperature reduction can reach 1-4°C, and the humidity increase can range from 3% to 8%. Lakes provide better regulatory effects than rivers. The study identified area, water depth, vegetation coverage, and built density as core influencing parameters. The three core scientific hypotheses proposed were experimentally validated: under the summer heat climate, the contribution of latent heat to cooling effects is no less than 60%, with an optimal water depth threshold of 0.8–1.2 m; shoreline sinuosity and vegetation coverage exhibit significant synergistic effects; and there is a clear thermodynamic transmission path between micro, meso, and macro scales.

(2) The thermodynamic mechanism of urban water body heat-moisture regulation with coupled landscape parameters was clarified. Latent heat evaporation is the dominant process for cooling in the summer heat period, contributing 60%–75%. Its intensity is co-regulated by water depth and vegetation coverage — appropriate water depth ensures evaporation driving force, and moderate vegetation reduces interface diffusion resistance. Radiation exchange contributes significantly in high-density building areas, where shoreline material albedo and building layout influence regulation effects by controlling shortwave radiation input and longwave radiation balance. Convective diffusion efficiency is dominated by water body shape and wind speed. Irregular water bodies can strengthen interface heat exchange, while high-density buildings tend to cause heat and humidity retention. The interactions between multiple parameters have clear thermodynamic origins of synergy or antagonism.

(3) The multi-scale thermodynamic transmission laws were clarified, and parameterization indicators and quantification standards were established with precise matching for each scale. The micro-scale is dominated by interface properties such as water body albedo and shoreline material conductivity for heat exchange efficiency. The meso-scale is dominated by form configuration parameters such as water body area, water depth, and shoreline sinuosity for block energy balance. The macro-scale is dominated by pattern parameters such as water body connectivity and green-blue space coupling for regional heat environment regulation. The scales achieve thermodynamic transmission through the "interface heat flux superposition-patch energy aggregation-regional energy accumulation" path.

(4) The multi-scale collaborative landscape design parameterization system and climate zone-specific design guidelines, verified through a case study in a summer-heat, winter-warm climate residential area, can achieve a 2.3°C reduction in daytime peak temperature, optimize the heat comfort index (PET) to below 35°C, increase the latent heat flux proportion to 63.5%, and improve the overall thermodynamic efficiency by 42.3%. This system breaks

through the traditional research bottleneck of "disconnection between mechanisms and parameters, scale confusion," achieving effective integration of thermodynamic precise regulation and engineering practice, and providing reliable thermodynamic theoretical support and practical technical solutions for urban microclimate optimization.

## REFERENCES

[1] Zanardi, F., Santunione, G., Despini, F., Sgarbi, E. (2025). Plants for a resilient city: The "climate-friendly parks" experiment in Reggio Emilia. Challenges in Sustainability, 13(4): 560-570. https://doi.org/10.56578/cis130407

[2] Norra, S. (2014). The biosphere in times of global urbanization. Journal of Geochemical Exploration, 147: 52-57. https://doi.org/10.1016/j.gexplo.2014.06.004

[3] Antomi, Y., Fajrin, Nofrianto, H., Defwaldi, Alhadi, Z. (2025). Dynamics of urban environment thermal comfort in Padang City based on remote sensing data measurements. International Journal of Environmental Impacts, 8(4): 755-764. https://doi.org/10.18280/ijei.080413

[4] Sakellaris, I.A., Saraga, D.E., Mandin, C., Roda, C., et al. (2016). Perceived indoor environment and occupants' comfort in European "modern" office buildings: The OFFICAIR study. International Journal of Environmental Research and Public Health, 13(5): 444. https://doi.org/10.3390/ijerph13050444

[5] Alcazar, S.S., Olivieri, F., Neila, J. (2016). Green roofs: Experimental and analytical study of its potential for urban microclimate regulation in Mediterranean–continental climates. Urban Climate, 17: 304-317. https://doi.org/10.1016/j.uclim.2016.02.004

[6] Wang, W., Zhang, B., Xiao, L., Zhou, W., Wang, H., He, X. (2018). Decoupling forest characteristics and background conditions to explain urban-rural variations of multiple microclimate regulation from urban trees. PeerJ, 6: e5450. https://doi.org/10.7717/peerj.5450

[7] Ampatzidis, P., Cintolesi, C., Kershaw, T. (2023). Impact of blue space geometry on urban heat island mitigation. Climate, 11(2): 28. https://doi.org/10.3390/cli11020028

[8] Masiero, É., de Souza, L.C.L. (2016). Improving urban thermal profile with trees and water features. Proceedings of the Institution of Civil Engineers-Urban Design and Planning, 169(2): 66-77. https://doi.org/10.1680/jurdp.14.00063

[9] Goeminne, R., Krause, S., Kaskel, S., Verstraelen, T., Evans, J.D. (2021). Charting the complete thermodynamic landscape of gas adsorption for a responsive metal-organic framework. Journal of the American Chemical Society, 143(11): 4143-4147. https://doi.org/10.1021/jacs.1c00522

[10] Wang, G.B., Zhang, X.R. (2020). Experimental performance comparison and trade-off among air-based precooling methods for postharvest apples by comprehensive multiscale thermodynamic analyses. International Journal of Energy Research, 44(3): 1546-1566. https://doi.org/10.1002/er.4919

[11] Świerk, D., Szpakowska, B. (2011). The effect of environmental factors on micropollutants in small water bodies. Ecological Chemistry and Engineering. S, 18(4): 545-569.

[12] Joniak, T., Kuczyńska-Kippen, N., Gąbka, M. (2017). Effect of agricultural landscape characteristics on the hydrobiota structure in small water bodies. Hydrobiologia, 793(1): 121-133. https://doi.org/10.1007/s10750-016-2913-5

[13] Hauser, F., Wastl-Walter, D., Weingartner, R. (2011). Integration of water bodies in the urban landscape-history, current status, and new challenges. Hydrologie und Wasserbewirtschaftung/Hydrology and Water Resources Management-Germany, 55(4): 199-214.

[14] Lim, J.S., Moon, K.H., Falchetto, A.C., Jeong, J.H. (2016). Testing and modelling of hygro-thermal expansion properties of concrete. KSCE Journal of Civil Engineering, 20(2): 709-717. https://doi.org/10.1007/s12205-015-0560-4

[15] Kadja, C.J.M., Dandonougbo, I., Korem, A., Adigbegnon, M., Teadoum Naringué, F., Allagbe, B.S. (2025). Urban expansion and its dual impact on biodiversity loss and thermal dynamics: A remote sensing-based assessment of Abomey-Calavi, Benin. Challenges in Sustainability, 13(3): 412-424. https://doi.org/10.56578/cis130307

[16] Tsochantaris, E., Muthachikavil, A.V., Peng, B., Liang, X., Kontogeorgis, G.M. (2022). Multiple insights call for revision of modern thermodynamic models to account for structural fluctuations in water. AIChE Journal, 68(11): e17891. https://doi.org/10.1002/aic.17891

[17] Fischer, S., Harangozó, D., Németh, D., Kocsis, B., Sysyn, M., Kurhan, D., Brautigam, A. (2024). Investigation of heat-affected zones of thermite rail weldings. Facta Universitatis, Series: Mechanical Engineering, 22(4): 689–710.

[18] Elek, G., Müller, M. (2024). Ervin Bauer's concept of biological thermodynamics and its different evaluations. Biosystems, 235: 105090. https://doi.org/10.1016/j.biosystems.2023.105090

[19] Wang, F., Zhou, B., Hu, J., Ye, C. (2021). Research on quantifiable target index system of distribution network planning for energy Internet. IEEE Access, 9: 136721-136735. https://doi.org/10.1109/ACCESS.2021.3117979

[20] Lei, N., Masanet, E. (2022). Climate-and technology-specific PUE and WUE estimations for US data centers using a hybrid statistical and thermodynamics-based approach. Resources, Conservation and Recycling, 182: 106323. https://doi.org/10.1016/j.resconrec.2022.106323